




Unveiling Asymptomatic Transmission: Analytical and Stability Insights of a Fractional-Order COVID-19 Model

Hatira Günerhan^a, Mohammad Sharif Ullah^b, Kottakkaran Sooppy Nisar^{c,d,g} , Waleed Adel^{e,f,*}

^a Department of Mathematics, Faculty of Education, Kafkas University, Kars, Turkey

^b Department of Mathematics, University of Tennessee at Chattanooga, Chattanooga, TN 37403, USA

^c Department of Mathematics, College of Science and Humanities in Alkharj, Prince Sattam Bin Abdulaziz University, Alkharj 11942, Saudi Arabia

^d Hourani Center for Applied Scientific Research, Al-Ahliyya Amman University, Jordan

^e School of Engineering and Applied Sciences, Nile University, Giza, 12588, Egypt

^f Department of Mathematics and Engineering Physics, Faculty of Engineering, Mansoura University, Mansoura, Egypt

^g Research Center of Applied Mathematics, Khazar University, Baku, Azerbaijan

ARTICLE INFO

Editor: Mohamed Fathy El-Amin Mousa

Keywords:

Caputo fractional derivative
Laplace Adomian decomposition
Coronavirus model
Stability

MSC 2020:

Primary: 26A33, 34D20

Secondary: 74G10

ABSTRACT

In this paper, we present a fractional-order SAIP epidemic model that incorporates asymptomatic transmission to jointly examine infection pathways and the influence of long-term memory effects. The Caputo fractional derivative is employed to capture the memory and hereditary characteristics intrinsic to real-world infectious disease dynamics, providing an alternative framework to traditional integer-order approaches. We establish key mathematical properties, including the positivity and boundedness of solutions, and derive the basic reproduction number. R_0 to determine thresholds for disease extinction or persistence. Both local and global stability analyses of the disease-free and endemic equilibria are conducted to clarify the conditions required for outbreak control. To address the complexities introduced by the fractional structure, we adapt the Laplace Adomian Decomposition Method (LADM) and demonstrate its effectiveness through detailed numerical simulations. The results show that variations in the fractional order affect epidemic trajectories, altering peak infection levels and duration, and thus emphasize the important role of memory effects in disease propagation.

Introduction

The COVID-19 pandemic, caused by the coronavirus SARS-CoV-2, has presented unprecedented global health, economic, and social challenges since its onset in late 2019 [1]. A distinguishing and aggravating aspect of COVID-19 is asymptomatic transmission, whereby infected persons who do not exhibit symptoms or are presymptomatic spread the virus to others [2,3]. Epidemiological studies [4–6] indicate that many illnesses originate from individuals who evade detection by symptom-based monitoring, testing, and contact tracing methods. This “silent spread” presents a significant challenge to control and requires a more profound understanding of its epidemiological effects. Mathematical modeling is fundamental to infectious disease research, providing insights into transmission

* Corresponding author.

E-mail addresses: gunerhanhatira@gmail.com (H. Günerhan), sharifju49@yahoo.com, kbc188@mocs.utc.edu (M.S. Ullah), n.sooppy@psau.edu.sa (K.S. Nisar), waleedadel@mans.edu.eg (W. Adel).

<https://doi.org/10.1016/j.sciaf.2025.e02929>

Received 24 May 2025; Received in revised form 15 August 2025; Accepted 26 August 2025

Available online 27 August 2025

2468-2276/© 2025 The Author(s). Published by Elsevier B.V. This is an open access article under the CC BY-NC-ND license (<http://creativecommons.org/licenses/by-nc-nd/4.0/>).

patterns, forecasting epidemic trajectories, and informing public health interventions [7]. Nevertheless, several initial COVID-19 models [8,9] either disregarded asymptomatic transmission or addressed it in a simplified manner, which may have resulted in an underestimation of the epidemic's actual magnitude and duration. Furthermore, most models rely on integer-order differential equations, which assume instantaneous transitions between compartments and overlook the biological memory effects inherent in disease processes. This memory indicates delayed behavioral reactions, fluctuations in immune system activity, or prolonged infectiousness over time. In recent years, fractional-order epidemic models [10–17] have gained recognition for their superior capacity to effectively represent the memory and genetic characteristics of disease dynamics compared to traditional integer-order models. The Caputo fractional derivative is preferred over other formulations due to its consistency with classical initial conditions, making it particularly suitable for simulating real-world biological processes. The Caputo derivative [18] provides a non-local operator that combines the historical states of the system, effectively capturing the history of disease transmission. In addition, the Adomian Decomposition Method (ADM) [19] offers a practical semi-analytical approach for solving the complex fractional differential equations that arise. ADM disaggregates the solution into a swiftly converging series and addresses nonlinear components with specifically formulated Adomian polynomials. The Caputo derivative and ADM combination enable the study of nonlinear epidemic models by providing explicit approximations of state variables, including susceptible, infected, and recovered populations, thereby enhancing our understanding of the long-term dynamics and stability of epidemic outbreaks.

Due to the Caputo fractional derivative's consistency and superior capacity to effectively represent the memory and genetic characteristics of disease, Ullah et al. [20] provide a mean-field approximation and fractional-order model integrated with the evolutionary game theory (EGT) framework for susceptible-vaccinated-infected-recovered (SVIR) epidemic dynamics, including artificial and natural immunity types. Olayiwola and Yunus [21] employ a Caputo-type fractional-order derivative operator to investigate the dynamics of dengue virus transmission within a host exhibiting adaptive immune responses. Hatira et al. [22] studied a fractional model of the HIV pandemic using the Caputo operator and the Constant Proportional Caputo (CPC) operator, respectively. Using the Caputo fractional order derivative, Ullah et al. [23] examine a comprehensive mathematical model for epidemic control strategies, including lockdown, self-protection, physical separation, quarantine, and isolation compartments. Olayiwola et al. [24] used the Caputo fractional order derivative to analyze its temporal dynamics, enabling the assessment of the memory effect that underlies financial stability and volatility over time. Yunus and Olayiwola [25] examine malaria, a widespread mosquito-borne disease in Africa that causes fever, chills, and headaches. Ongun [26] employs the Laplace Adomian Decomposition Method to obtain an approximate solution for systems of nonlinear ordinary differential equations, exemplified by a model for HIV infection of $CD4^+$ T cells. Yunus and Olayiwola [27] propose an innovative mathematical framework for addressing Ebola and malaria issues in Sub-Saharan Africa, integrating the Laplace transformation with the Caputo fractional order derivative. Haq et al. [28] investigated the fractional order smoking cessation model's analytical solution (approximate solution) using the Laplace transformation. Yunus et al. [29] investigated a fractional-order model of Lassa disease using the Laplace-Adomian Decomposition Method. Baleanu et al. [30] present a fractional-order epidemic model for pediatric disorders, utilizing the fractional derivative technique introduced by Caputo and Fabrizio, along with the Laplace Adomian decomposition method (LADM). Gaxiola and Biswas [31] use the Laplace-Adomian decomposition method to illustrate numerical dispersive bright and dark optical solitons represented by the Radhakrishnan-Kundu-Lakshmanan equation. Yunus and Olayiwola [32] examine the pivotal significance of COVID-19 immunizations in controlling the epidemic, particularly in Nigeria. Hatira et al. [33] offer a nonlinear fractional smoking mathematical model with a modified version of the Caputo fractional-order derivative. Analytical and approximate-analytical solutions for the proposed mathematical model are derived using the fractional differential transform technique (FDTM) and the Laplace Adomian decomposition method (LADM). Olayiwola et al. [34] evaluate the efficacy of current innovations in COVID-19 therapy, particularly antiviral agents and monoclonal antibodies, in mitigating the transmission of the virus. Yunus et al. [35] studied the viral dynamics of Lassa fever, primarily seen in West Africa, through a fractional order model. The model's analytical solution is derived using the Laplace Adomian Decomposition Method (LADM) as an infinite series that rapidly converges to its precise value.

Several studies have incorporated fractional calculus into COVID-19 models to capture memory effects in transmission dynamics. For instance, Zhang et al. [36] developed a fractional SEIR-type model with asymptomatic carriers, while Ndaïrou et al. [1] extended a COVID-19 model to include fractional dynamics with asymptomatic compartments, analyzing their stability and numerical behavior. Building on these studies, our work adapts and extends existing approaches to a fractional-order SAIP COVID-19 framework. While previous studies have considered fractional models with asymptomatic compartments, the SAIP provides a distinct compartmental arrangement that allows explicit modeling of protected individuals alongside asymptomatic and symptomatic infectious populations. Thus, our aim in this study is to reveal the influence of asymptomatic carriers on epidemic persistence and control needs some additional work, providing theoretical insights and computational evidence to enhance public health strategies. Our model integrates fractional calculus with intricate disease compartmentalization, offering a good understanding of the memory-dependent and asymptomatic-driven dynamics of COVID-19 and potentially other analogous viral diseases. However, this introduces notable challenges: the nonlocal nature of the Caputo operator complicates mathematical analysis, requiring careful construction of Lyapunov functions to establish global stability; the combined inclusion of asymptomatic compartments and fractional terms increases system dimensionality, precluding closed-form solutions and necessitating approximate analytical techniques such as the Laplace Adomian Decomposition Method (LADM); and finally, the model exhibits high sensitivity to variations in fractional order and asymptomatic transmission parameters, underscoring both the richness and analytical complexity of the dynamics. Our rigorous investigation of positivity, boundedness, and stability, supported by detailed simulations, demonstrates how fractional memory and silence spread jointly shape epidemic peaks and durations. Altogether, this comprehensive framework advances theoretical epidemic modeling and establishes a robust platform for future extensions involving vaccination, spatial heterogeneity, or stochastic effects to better inform public health decision-making. The novelty of the paper lies in the following points:

1. A fractional-order SIR model is developed to simulate the spread dynamics of the COVID-19 pandemic, capturing memory and hereditary effects that classical integer-order models overlook.
2. A modified fractional SAIP model is proposed, explicitly incorporating asymptomatic individuals $A(t)$ and protected individuals $P(t)$ providing a more comprehensive framework to reveal complex transmission dynamics unique to COVID-19.
3. Both the fractional SIR and the enhanced SAIP models are analyzed and solved using an adapted Laplace Adomian Decomposition Method (LADM), enabling the derivation of efficient approximate analytical solutions despite the models' nonlocal nature.
4. Numerical simulations are performed for different fractional orders, specifically $\alpha = 0.5, 0.75$, demonstrating how fractional memory significantly influences infection peaks and duration, and confirming the models' capability to reflect the primary characteristics of COVID-19 outbreaks, and compared with the ODE45 code for validation and real data from Portugal.
5. The proposed method is straightforward to implement yet yields accurate results, illustrating its effectiveness in studying fractional epidemic systems and highlighting its potential as a tool for broader epidemiological applications.

The paper's organization is as follows: Section 2 discusses the model formulation, whereas Section 3 presents some basic definitions of fractional operators. The positivity and boundedness of the solution to the main system are discussed in Section 4. Section 5 investigates the stability and equilibrium points. The existence of a uniformly stable solution is provided in Section 6, while the main steps for the Laplace Adomian decomposition method are illustrated in Section 7. Numerical simulations to verify the theoretical findings and compare them with real-world data are presented in Section 8. Section 9 highlights a conclusion for the study and future work.

Basic Definitions

This section presents fundamental definitions and properties from fractional calculus theory that will be used in the subsequent analysis.

Definition 2.1. A real function $f(x)$, $x > 0$ is said to be in the space C_μ , $\mu \in \mathbb{R}$ if there exists a real number $P > \mu$ such that $f(x) = x^P f_1(x)$ where $f_1(x) \in C[0, \infty)$. Clearly $C_\mu < C_\beta$ if $\mu < \beta$.

Definition 2.2. A function $f(x)$, $x > 0$ is said to be in the space C_μ^m , $m \in \mathbb{N} \setminus \{0\}$ if $f^{(m)} \in C_\mu$.

Definition 2.3. [37] The Riemann-Liouville fractional integral operator of the order $\alpha > 0$ of a function, $f \in C_\mu$, $\mu \geq -1$ is defined as

$$(J_a^\alpha f)(x) = \frac{1}{\Gamma(\alpha)} \int_a^x (x - \tau)^{\alpha-1} f(\tau) d\tau, x > a, \tag{2.1}$$

$$(J_a^0 f)(x) = f(x). \tag{2.2}$$

All the properties of the operator J^α can be found in [18], we mention only the following, for $f \in C_\mu$, $\mu \geq -1$, $\alpha, \beta \geq 0$, and $\gamma > -1$ we have

$$(J_a^\alpha J_a^\beta f)(x) = (J_a^{\alpha+\beta} f)(x), \tag{2.3}$$

$$(J_a^\alpha J_a^\beta f)(x) = (J_a^\beta J_a^\alpha f)(x) \tag{2.4}$$

$$J_a^\alpha x^\gamma = \frac{\Gamma(\gamma + 1)}{\Gamma(\alpha + \gamma + 1)} x^{\alpha+\gamma}. \tag{2.5}$$

The Riemann-Liouville fractional derivative is often preferred for simulations because of its computational advantages. However, in this work, we adopt a modified version of the fractional operator D_a^α , introduced by Caputo in [18], which offers more practical benefits for modeling physical problems. This definition is given as follows:

Definition 2.4. [18] The fractional derivative of the function $f(x)$ in Caputo's sense is defined as

$$\left(D_a^\alpha f \right)(x) = \left(J_a^{m-\alpha} D_a^m f \right)(x) = \frac{1}{\Gamma(m-\alpha)} \int_a^x (x-t)^{m-\alpha-1} f^{(m)}(t) dt, \text{ for } m-1 < \alpha < m, m \in \mathbb{N}, x > 0. \tag{2.6}$$

Lemma 2.1. If $-1 < \alpha < m$, $m \in \mathbb{N}$ and $\mu \geq -1$, then

$$(J_a^\alpha D_a^\alpha f)(x) = f(x) - \sum_{k=0}^{m-1} f^{(k)}(a) \left(\frac{(x-a)^k}{k!} \right), a \geq 0 \tag{2.7}$$

$$(D_a^\alpha J_a^\alpha f)(x) = f(x) \tag{2.8}$$

Next, we will provide the proposed model in detail.

Model formulation

Mathematical epidemic models are essential for understanding and forecasting the transmission of infectious diseases across populations. Typically, these models use differential equations to accurately represent how infections spread. It also includes population demographics, disease features, and intervention options. Formulating such models requires the specification of variables to represent distinct population compartments (such as susceptible, asymptomatic, infected, and recovered individuals), as well as determining parameters to measure transmission and recovery rates that depict the dynamics of these compartments over time. Using mathematical analysis and computer simulations, these models provide vital insights into the fundamental processes that drive epidemics and, in turn, aid public health professionals in developing effective control strategies and mitigating the consequences of infectious diseases. The proposed fractional SAIP model can take the following form:

$$\begin{aligned}
 D_a^\alpha S(t) &= [-\beta(1-\rho)(\theta A(t) + I(t)) - \varphi\rho]S(t) + \omega P(t), \\
 D_a^\alpha A(t) &= \beta(1-\rho)(\theta A(t) + I(t))S(t) - \nu A(t), \\
 D_a^\alpha I(t) &= \nu A(t) - \delta I(t), \\
 D_a^\alpha P(t) &= \varphi\rho S(t) - \omega P(t),
 \end{aligned}
 \tag{3.1}$$

With the following initial conditions

$$S(0) = H_1, I(0) = H_2, A(0) = H_3, P(0) = H_4.$$

From Eq. (3.1), the total population is divided into four categories. These categories associated with the system (3.1) can be summarized in Table 1. Additionally, the initial conditions and parameter values for system (3.1) are listed in Table 2. These values of the parameters and initial conditions were taken according to the data for Portugal from March 2, 2020, to June 19, 2020 [38]. Additionally, the interaction between different compartments for model (3.1) is illustrated in Figure 1.

Next, we describe the terms of interaction. The interaction terms collectively define the movement of individuals through different states in the SAIP model, providing insights into the progression of infection, the role of asymptomatic carriers, the development of immunity, and the dynamics of virus transmission within the population. The following state interactions are as follows

1. $S \rightarrow A$ (Susceptible to Asymptomatic): This interaction term represents the movement of susceptible individuals to the asymptomatic compartment. It signifies that susceptible individuals become asymptomatic upon infection with the virus but do not display symptoms.
2. $S \rightarrow I$ (Susceptible to Infected): This term describes the transition of susceptible individuals to the infected compartment. It occurs when susceptible individuals come into contact with infectious individuals and become infected themselves. This transition is influenced by factors like the virus's transmission rate and the frequency of contact between susceptible and infectious individuals.
3. $A \rightarrow I$ (Asymptomatic to Infected): This interaction term signifies the movement of asymptomatic individuals to the infected compartment. Asymptomatic individuals, although not displaying symptoms, can still transmit the virus to others, thus transitioning to the infected state.
4. $I \rightarrow P$ (Infected to Protected): This interaction term represents the transition of infected individuals to the protected compartment. Infected individuals recover from the virus, gaining immunity and becoming protected against future infections. This transition may also include individuals who acquire immunity through vaccination.
5. $I \rightarrow I$ (Infected to Infected): This term accounts for interactions among infected individuals, such as secondary transmissions within the population. It reflects the ongoing transmission dynamics of the virus within the community, capturing the spread of infection from one infected individual to another.

Positivity and boundedness of the solutions

In this section, we will provide details proving the positive and boundedness of the proposed model. The model can be expressed in the following form:

Table 1
Description and initial values of variables in the system (3.1).

State	Definition	Initial conditions [38]
$S(t)$	Susceptible individuals	1
$A(t)$	Asymptomatic individuals	1.29×10^{-6}
$I(t)$	Confirmed/active infected individuals	1.92×10^{-7}
$P(t)$	Protected/prevented individuals	0

Table 2
Specification of the parameters and initial values used in system (3.1).

Parameter	Definition	Value [38]
N	Total number of populations	10295909
β	Transmission rate	1.492
θ	Modification parameter	1
ρ	Fraction of susceptible S transferred to the protected class P	0.675
ϕ	The transition rate of susceptible S to the protected class P	1/12
ω	The transition rate of protected P to susceptible S	1/45
ν	The rate at which asymptomatic individuals A progress to the confirmed infectious class I	0.15
δ	The rate at which confirmed infected individuals I move into the recovered or removed category R	1/30

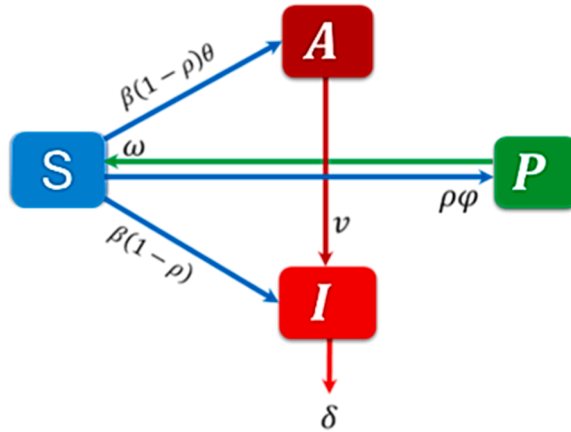


Fig. 1. Schematic diagram of the presented model (2).

$$\begin{aligned}
 D_t^\alpha S(t) &= [-\beta(1-\rho)(\theta A(t) + I(t)) - \phi\rho]S(t) + \omega P(t), \\
 D_t^\alpha A(t) &= \beta(1-\rho)(\theta A(t) + I(t))S(t) - \nu A(t), \\
 D_t^\alpha I(t) &= \nu A(t) - \delta I(t), \\
 D_t^\alpha P(t) &= \phi\rho S(t) - \omega P(t),
 \end{aligned}
 \tag{4.1}$$

Where $I(t) \geq I^0 e^{-\delta t}, \forall t \geq 0, P(t) \geq P^0 e^{-\omega t}, \forall t \geq 0$.

Hence, we get the following for D_φ where $\varphi \in D_\varphi$ as in [39]

$$\| \varphi \|_\infty = \sup_{t \in D_\varphi} |\varphi(t)|
 \tag{4.2}$$

Next, by using the overhead norm, $A(t)$ and $S(t)$ can be as follows

$$\dot{A} = \beta(1-\rho)(\theta A + I)S - \nu A, \forall t \geq 0 \geq \{\beta(1-\rho)\theta S - \nu\}A, \forall t \geq 0 \geq \{\beta(1-\rho)\theta \sup_{t \in D_S} |S| - \nu\}A, \forall t \geq 0 \geq$$

$$\{\beta(1-\rho)\theta \|S\|_\infty - \nu\}A, \forall t \geq 0.
 \tag{4.3}$$

Therefore,

$$A(t) \geq A^0 e^{\{\beta(1-\rho)\theta \|S\|_\infty - \nu\}t}, \forall t \geq 0.
 \tag{4.4}$$

In the same way, the susceptible class can be in the form

$$S(t) \geq S^0 e^{-[\beta(1-\rho)(\theta \|A\|_\infty + \|I\|_\infty) + \phi\rho]t}, \forall t \geq 0.
 \tag{4.5}$$

Finally, we conclude that the solution is both positive and bounded. In the next section, we will investigate the existence of the equilibrium points for the proposed system.

Stability analysis and equilibrium points

In this section, we will illustrate the existence of the equilibrium points for the model (2). We seek to find the two equilibrium points, named the Disease-free equilibrium (DFE) and Endemic equilibrium (EE) points. First, we investigate the DFE point.

Existence of Disease-free equilibrium (DFE) point

In this subsection, we will prove the existence of the Disease-Free Equilibrium (DFE). To evaluate this point, we put $I = 0$ in the system (3.1), which will provide the point in the following form $E_0 = (S^0, A^0, I^0, A^0) = (N, 0, 0, 0)$. Here, $0 \leq S^0 \leq 1$.

Basic reproduction R_0 number and effective reproduction number R_e

To proceed with our preliminary investigation, we will examine the calculation of the basic reproduction number, R_0 , which is significant for epidemiological modeling, as it has been demonstrated to assist in understanding stable circumstances. If this value is less than 1, local stability is expected; instability will be foreseen if it is greater than 1. To arrive at the reproduction value in this case, we will utilize the next-generation matrix [40] technique as follows:

$$F = \begin{bmatrix} \beta(1-\rho)\theta & \beta(1-\rho) \\ 0 & 0 \end{bmatrix}, \quad V = \begin{bmatrix} \nu & 0 \\ -\nu & \delta \end{bmatrix}. \tag{5.1}$$

Then,

$$FV^{-1} = \frac{1}{\delta\nu} \begin{bmatrix} \delta\beta(1-\rho)\theta + \beta(1-\rho)\nu & \beta(1-\rho)\nu \\ 0 & 0 \end{bmatrix} \tag{5.2}$$

The basic reproduction number can be evaluated in the form

$$R_0 = \frac{\beta(1-\rho)\theta}{\nu} + \frac{\beta(1-\rho)}{\delta}. \tag{5.3}$$

We will get the maximum reproductive number values when the transmission rate is high. In addition, the effective reproduction number R_e is

$$R_e(t) = \left[\frac{\beta(1-\rho)\theta}{\nu} + \frac{\beta(1-\rho)}{\delta} \right] S(t). \tag{5.4}$$

Thus, we arrive at the following theorem

Theorem 5.1. If $R_0 < 1$, then the DFE (E_0) is locally asymptotically stable. Conversely, if $R_0 > 1$, the disease-free equilibrium is unstable.

Proof. We now proceed to compute the Jacobian matrix of the proposed model, given by:

$$J = \begin{bmatrix} -\beta(1-\rho)(\theta A + I) - \varphi\rho & -\beta(1-\rho)\theta S & -\beta(1-\rho)S & \omega \\ \beta(1-\rho)(\theta A + I) & \beta(1-\rho)\theta S - \nu & \beta(1-\rho)S & 0 \\ 0 & \nu & -\delta & 0 \\ \varphi\rho & 0 & 0 & -\omega \end{bmatrix}, \tag{5.5}$$

Then, we obtain

$$J(E_0) = \begin{bmatrix} -\varphi\rho & -\beta(1-\rho)\theta & -\beta(1-\rho) & \omega \\ 0 & \beta(1-\rho)\theta - \nu & \beta(1-\rho) & 0 \\ 0 & \nu & -\delta & 0 \\ \varphi\rho & 0 & 0 & -\omega \end{bmatrix}. \tag{5.6}$$

The characteristic equation $|J(E_0) - \lambda I| = 0$ has four roots, which can be summarized in the form

$$\begin{aligned} \lambda_1 &= 0, \\ \lambda_2 &= -\varphi\rho - \omega, \\ \lambda_3 &= \frac{1}{2} \left(-\nu - \delta + \beta\theta - \beta\theta\rho - \sqrt{(\nu + \delta - \beta\theta + \beta\theta\rho)^2 - 4(-\nu\beta + \nu\delta - \beta\delta\theta + \nu\beta\rho + \beta\delta\theta\rho)} \right), \\ \lambda_4 &= \frac{1}{2} \left(-\nu - \delta + \beta\theta - \beta\theta\rho + \sqrt{(\nu + \delta - \beta\theta + \beta\theta\rho)^2 - 4(-\nu\beta + \nu\delta - \beta\delta\theta + \nu\beta\rho + \beta\delta\theta\rho)} \right). \end{aligned}$$

It can be noted that the first two eigenvalues are negative or equal to zero, and the second two's real parts are negative; then, by applying the Routh-Hurwitz criteria [7], we conclude that the model is locally asymptotically stable at E_0 when $R_0 < 1$ and unstable whenever $R_0 > 1$. ■

Next, we examine the existence of the endemic equilibrium point.

Existence of Endemic equilibrium point (EE)

In this part, we look into whether the endemic equilibrium is denoted by $E_* = (S^*, A^*, I^*, P^*)$ Exists. In contrast to the demographic and SIS models, this model considers the non-demographic epidemic scenario, in which the epidemic process proceeds unilaterally ($S \rightarrow A \rightarrow I \rightarrow P$). Then, for the endemic equilibrium point model, equations are given by

$$\begin{aligned} [-\beta(1-\rho)(\theta A + I) - \varphi\rho]S + \omega P &= 0, \\ \beta(1-\rho)(\theta A + I)S - \nu A &= 0, \\ \nu A - \delta I &= 0, \\ \varphi\rho S - \omega P &= 0. \end{aligned} \tag{5.7}$$

When $t \rightarrow \infty$, we get, $A(\infty) \rightarrow 0$, $I(\infty) \rightarrow 0$ and $S(\infty) + P(\infty) = 1$.

Theorem 4.2. The proposed asymptomatic carrier-based coronavirus model (3.1) is globally asymptotically stable at E_0 when $R_0 \leq 1$.

Proof. To establish the global stability of the current asymptomatic carrier model, we propose a Lyapunov function defined as follows:

$$L_f = g_1 A + g_2 I, \tag{5.8}$$

where g_i for $i = 1, 2$ are arbitrary constants.

When considering differentiation on both sides of equation (5.8), one may express it as,

$$\dot{L}_f = g_1 \dot{A} + g_2 \dot{I} = [\beta(1-p)(\theta A + I)S - \nu A] + g_2 [\nu A - \delta I].$$

The above equation can be simplified as follows:

$$\dot{L} = [g_1\beta(1-p)S - g_2\delta]I + [g_1\beta\theta(1-p)S - g_1\nu + g_2\nu]A. \tag{5.9}$$

Assume,

$$g_1 = 1, g_2 = \frac{\beta(1-p)S}{\delta}.$$

By replacing the values for the arbitrary variables in equation (5.9), one obtains

$$\dot{L} = \nu \left[\frac{\beta(1-\rho)\theta}{\nu} + \frac{\beta(1-\rho)}{\delta} - 1 \right] A = \nu[R_0 - 1]A.$$

There is compelling evidence that when R_0 is less than or equal to 1, then \dot{L} is less than or equal to 0. Furthermore, when the derivative of L is zero, A is also zero. When A is set to 0 in the present nonlinear system (3.1) and as time approaches infinity, the variables (S, A, I, P) converge to the disease-free equilibrium point $(N, 0, 0, 0)$. Therefore, the equilibrium point E_0 , which is disease-free, and will show the most significant invariant set. When R_0 is less than or equal to 1, according to LaSalle’s invariance principle [20,23, 39], the suggested model is globally asymptotically stable inside the feasible domain Ω .

Existence of a uniformly stable solution

In this section, we present a detailed proof of the exactness of the solution to the main model. To demonstrate the exactness of a uniformly stable solution, we begin by assuming that:

$$\begin{aligned} \dot{S} &= \{-\beta(1-\rho)(\theta A + I) - \varphi\rho\}S + \omega P = f_1(S, A, I, P) \\ \dot{A} &= \beta(1-\rho)(\theta A + I)S - \nu A = f_2(S, A, I, P) \\ \dot{I} &= \nu A - \delta I = f_3(S, A, I, P) \\ \dot{P} &= \varphi\rho S - \omega P = f_4(S, A, I, P) \end{aligned} \tag{6.1}$$

For the total population $N(t)$, we may write the domain in the following form

$$\Pi = \{(S(t) + A(t) + I(t) + P(t)) \in \mathbb{R}^4 : |\zeta(i)| \leq N(t), t \in [0, T]. \tag{6.2}$$

Thus, over Π , we have

$$\begin{aligned}
 \frac{\partial f_1}{\partial S} &= -\beta(1-\rho)(\theta A + I) - \varphi\rho \Rightarrow \left| \frac{\partial f_1}{\partial S} \right| \leq a_{11}, \frac{\partial f_1}{\partial A} = -\beta(1-\rho)\theta S \Rightarrow \left| \frac{\partial f_1}{\partial A} \right| \leq a_{12}, \\
 \frac{\partial f_1}{\partial I} &= -\beta(1-\rho)S \Rightarrow \left| \frac{\partial f_1}{\partial I} \right| \leq a_{13}, \frac{\partial f_1}{\partial P} = \omega \Rightarrow \left| \frac{\partial f_1}{\partial P} \right| \leq a_{14}, \\
 \frac{\partial f_2}{\partial S} &= \beta(1-\rho)(\theta A + I) \Rightarrow \left| \frac{\partial f_2}{\partial S} \right| \leq a_{21}, \frac{\partial f_2}{\partial A} = \beta(1-\rho)\theta S - \nu \Rightarrow \left| \frac{\partial f_2}{\partial A} \right| \leq a_{22}, \\
 \frac{\partial f_2}{\partial I} &= \beta(1-\rho)S \Rightarrow \left| \frac{\partial f_2}{\partial I} \right| \leq a_{23}, \frac{\partial f_2}{\partial P} = 0 = f_2(P) = a_{24}, \\
 \frac{\partial f_3}{\partial S_1} &= 0 = f_3(S) = a_{31}, \frac{\partial f_3}{\partial A} = \nu \Rightarrow \left| \frac{\partial f_3}{\partial A} \right| \leq a_{32}, \\
 \frac{\partial f_3}{\partial I} &= -\delta \Rightarrow \left| \frac{\partial f_3}{\partial I} \right| \leq a_{33}, \frac{\partial f_3}{\partial P} = 0 = f_3(P) = a_{34}, \\
 \frac{\partial f_4}{\partial S} &= \varphi\rho \Rightarrow \left| \frac{\partial f_4}{\partial S} \right| \leq a_{41}, \frac{\partial f_4}{\partial A} = 0 = f_4(A) = a_{42}, \\
 \frac{\partial f_4}{\partial I} &= 0 = f_4(I) = a_{43}, \frac{\partial f_4}{\partial P} = -\omega \Rightarrow \left| \frac{\partial f_4}{\partial P} \right| \leq a_{44},
 \end{aligned} \tag{6.3}$$

Here, a_{ij} ($i \geq 1$ and $j \leq 4$) all have positive values. Therefore, the four functions in the model, namely f_1, f_2, \dots, f_4 all are satisfied with the well-known Lipchitz condition [31,41]. Lastly, we can say that all functions are continuous.

Next, we shall verify the theoretical findings by finding the analytical solution using the Laplace-Adomian decomposition Method.

Laplace Adomian Decomposition Method

This section outlines the fundamental steps of the Laplace Adomian Decomposition Method (LADM), beginning with the necessary preliminary definitions.

Definition 6.1. [36] A function defined on the interval $0 \leq t < \infty$ is said to be exponentially bounded of order $\sigma \in R$ if it satisfies an inequality of the form $\|f(t)\| \leq Me^{\sigma t}$, for some real constant $M > 0$.

To find an analytical solution to model (3.1), we first apply the Laplace transform to both sides of Eq. (3.1) in the following form.

$$\begin{aligned}
 L\left(\frac{d^\alpha S}{dt^\alpha}\right) &= -\beta(1-\rho)\theta L(A(t)S(t)) - \beta(1-\rho) L(I(t)S(t)) - \varphi\rho L(S(t)) + \omega L(P(t)), \\
 L\left(\frac{d^\alpha A}{dt^\alpha}\right) &= \beta(1-\rho)\theta L(A(t)S(t)) + \beta(1-\rho) L(I(t)S(t)) - \nu L(A(t)), \\
 L\left(\frac{d^\alpha I}{dt^\alpha}\right) &= \nu L(A(t)) - \delta L(I(t)), \\
 L\left(\frac{d^\alpha P}{dt^\alpha}\right) &= \varphi\rho L(S(t)) - \omega L(P(t)),
 \end{aligned} \tag{7.1}$$

Then, by applying the definition of the Caputo fractional derivative for Eq. (7.1), we get

$$\begin{aligned}
 s^\alpha L(S) - s^{\alpha-1}S(0) &= -\beta(1-\rho)\theta L(A(t)S(t)) - \beta(1-\rho) L(I(t)S(t)) - \varphi\rho L(S(t)) + \omega L(P(t)), \\
 s^\alpha L(A) - s^{\alpha-1}A(0) &= \nu L(A(t)) - \delta L(I(t)), \\
 s^\alpha L(P) - s^{\alpha-1}P(0) &= \varphi\rho L(S(t)) - \omega L(P(t)).
 \end{aligned} \tag{7.2}$$

Next, by substituting the initial conditions in Eq. (2) into the model (7.2), we get

$$\begin{aligned}
 L(S) &= \frac{S(0)}{s} - \frac{\beta(1-\rho)\theta}{s^\alpha} L(A(t)S(t)) - \frac{\beta(1-\rho)}{s^\alpha} L(I(t)S(t)) - \frac{\varphi\rho}{s^\alpha} L(S(t)) + \frac{\omega}{s^\alpha} L(P(t)), \\
 L(A) &= \frac{A(0)}{s} + \frac{\beta(1-\rho)\theta}{s^\alpha} L(A(t)S(t)) + \frac{\beta(1-\rho)}{s^\alpha} L(I(t)S(t)) - \frac{\nu}{s^\alpha} L(A(t)), \\
 L(I) &= \frac{I(0)}{s} + \frac{\nu}{s^\alpha} L(A(t)) - \frac{\delta}{s^\alpha} L(I(t)), \\
 L(P) &= \frac{P(0)}{s} + \frac{\varphi\rho}{s^\alpha} L(S(t)) - \frac{\omega}{s^\alpha} L(P(t)).
 \end{aligned} \tag{7.3}$$

The proposed method expresses the solution as an infinite series. To facilitate the application of the Adomian Decomposition Method, let $F = I S$ and $M = A S$. Accordingly, we represent the solution in the form of an infinite series as follows:

$$S = \sum_{n=0}^{\infty} s_n, A = \sum_{n=0}^{\infty} A_n, I = \sum_{n=0}^{\infty} I_n, P = \sum_{n=0}^{\infty} P_n. \tag{7.4}$$

Then, by decomposing the nonlinear part named F and M in the following form

$$F = \sum_{n=0}^{\infty} F_n, M = \sum_{n=0}^{\infty} M_n, \tag{7.5}$$

Here, F_n and M_n can be computed using the convolution operation as

$$F_n = \frac{1}{\Gamma(n+1)} \frac{d^n}{d\eta^n} \left[\sum_{i=0}^n \eta^i I_i \sum_{i=0}^n \eta^i S_i \right]_{\eta=0},$$

$$M_n = \frac{1}{\Gamma(n+1)} \frac{d^n}{d\eta^n} \left[\sum_{i=0}^n \eta^i A_i \sum_{i=0}^n \eta^i S_i \right]_{\eta=0}, \tag{7.6}$$

By substituting Eq. (7.4-7.6) into Eq. (7.3), we have resulted in the form:

$$L\left(\sum_{n=0}^{\infty} s_n\right) = \frac{S(0)}{s} - \frac{\beta(1-\rho)\theta}{s^\alpha} L\left(\sum_{n=0}^{\infty} M_n\right) - \frac{\beta(1-\rho)}{s^\alpha} L\left(\sum_{n=0}^{\infty} F_n\right) - \frac{\varphi\rho}{s^\alpha} L\left(\sum_{n=0}^{\infty} S_n\right) + \frac{\omega}{s^\alpha} L\left(\sum_{n=0}^{\infty} P_n\right),$$

$$L\left(\sum_{n=0}^{\infty} A_n\right) = \frac{A(0)}{s} + \frac{\beta(1-\rho)\theta}{s^\alpha} L\left(\sum_{n=0}^{\infty} M_n\right) + \frac{\beta(1-\rho)}{s^\alpha} L\left(\sum_{n=0}^{\infty} F_n\right) - \frac{\nu}{s^\alpha} L\left(\sum_{n=0}^{\infty} A_n\right),$$

$$L\left(\sum_{n=0}^{\infty} I_n\right) = \frac{I(0)}{s} + \frac{\nu}{s^\alpha} L\left(\sum_{n=0}^{\infty} A_n\right) - \frac{\delta}{s^\alpha} L\left(\sum_{n=0}^{\infty} I_n\right),$$

$$L\left(\sum_{n=0}^{\infty} P_n\right) = \frac{P(0)}{s} + \frac{\varphi\rho}{s^\alpha} L\left(\sum_{n=0}^{\infty} S_n\right) - \frac{\omega}{s^\alpha} L\left(\sum_{n=0}^{\infty} P_n\right). \tag{7.7}$$

By equating both sides of Eq. (7.7), we derive the following iterative algorithm:

$$L(S_0) = \frac{S(0)}{s}, L(A_0) = \frac{A(0)}{s}, L(I_0) = \frac{I(0)}{s}, L(P_0) = \frac{P(0)}{s},$$

$$L(s_1) = -\frac{\beta(1-\rho)\theta}{s^\alpha} L(M_0) - \frac{\beta(1-\rho)}{s^\alpha} L(F_0) - \frac{\varphi\rho}{s^\alpha} L(s_0) + \frac{\omega}{s^\alpha} L(P_0), L(A_1) = \frac{\beta(1-\rho)\theta}{s^\alpha} L(M_0) + \frac{\beta(1-\rho)}{s^\alpha} L(F_0) - \frac{\nu}{s^\alpha} L(A_0),$$

$$L(I_1) = \frac{\nu}{s^\alpha} L(A_0) - \frac{\delta}{s^\alpha} L(I_0), L(P_1) = \frac{\varphi\rho}{s^\alpha} L(s_{1,0}) - \frac{\omega}{s^\alpha} L(P_0), \dots$$

$$L(s_n) = -\frac{\beta(1-\rho)\theta}{s^\alpha} L(M_{n-1}) - \frac{\beta(1-\rho)}{s^\alpha} L(F_{n-1}) - \frac{\varphi\rho}{s^\alpha} L(s_{n-1}) + \frac{\omega}{s^\alpha} L(P_{n-1}),$$

$$L(A_n) = \frac{\beta(1-\rho)\theta}{s^\alpha} L(M_{n-1}) + \frac{\beta(1-\rho)}{s^\alpha} L(F_{n-1}) - \frac{\nu}{s^\alpha} L(A_{n-1}),$$

$$L(I_n) = \frac{\nu}{s^\alpha} L(A_{n-1}) - \frac{\delta}{s^\alpha} L(I_{n-1}),$$

$$L(P_n) = \frac{\varphi\rho}{s^\alpha} L(s_{n-1}) - \frac{\omega}{s^\alpha} L(P_{n-1}). \tag{7.8}$$

Finally, applying the inverse transform to Eq. (7.8) yields the following expression:

$$S_0 = S(0), A_0 = A(0), I_0 = I(0), R_0 = R(0),$$

$$S = [-\beta(1-\rho)\theta M_0 - \beta(1-\rho)F_0 - \varphi\rho S_0] \frac{t^\alpha}{\Gamma(\alpha+1)},$$

$$A_1 = [\beta(1-\rho)\theta M_0 + \beta(1-\rho)F_0 - \nu A_0] \frac{t^\alpha}{\Gamma(\alpha+1)},$$

$$I_1 = [\nu A_0 - \delta I_0] \frac{t^\alpha}{\Gamma(\alpha+1)}, P_1 = [\varphi\rho S_0 - \omega P_0] \frac{t^\alpha}{\Gamma(\alpha+1)}, \dots \tag{7.9}$$

Similarly, the remaining terms can be derived, leading to the final solution expressed as an infinite series, as shown in Eq. (7.4). The solution obtained in Eq. (7.9) provides the values of the state variables for the SAIP model described in Eq. (1.1). These analytical results will be validated through numerical simulations presented in the following section.

Results and discussions

Numerical Simulations

In this section, we analyze the results obtained from solving the fractional SAIP model described in system (2.1) for various values of the fractional order α , as well as different values of the parameters β (transmission rate) and ρ (protection rate). The results obtained by ALDM match the exact solutions when $\alpha = 1$. Figures 2, 3, and 4 provide a comparison between the results obtained by LADM and

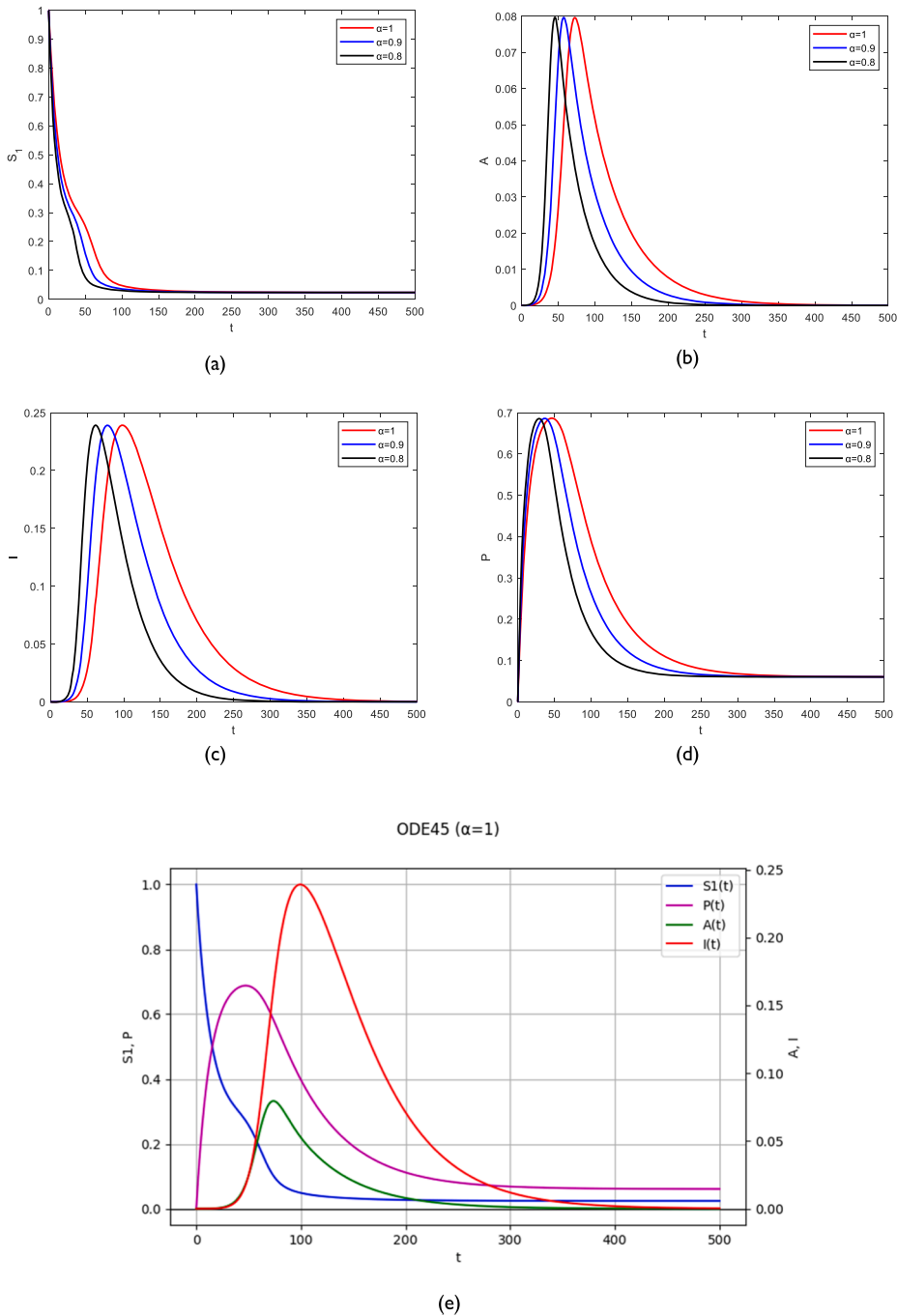


Fig. 2. Simulation of model (2.1) compartments: (a) Susceptible $S(t)$, (b) Asymptomatic $A(t)$, (c) Infected $I(t)$ and Protected $P(t)$ for different values of α , obtained using LADM. The results obtained by ODE45 for $\alpha = 1$ (e) are also shown, with $\beta_1 = 1.492$, $\rho_1 = 0.675$ and $0 \leq t \leq 500$.

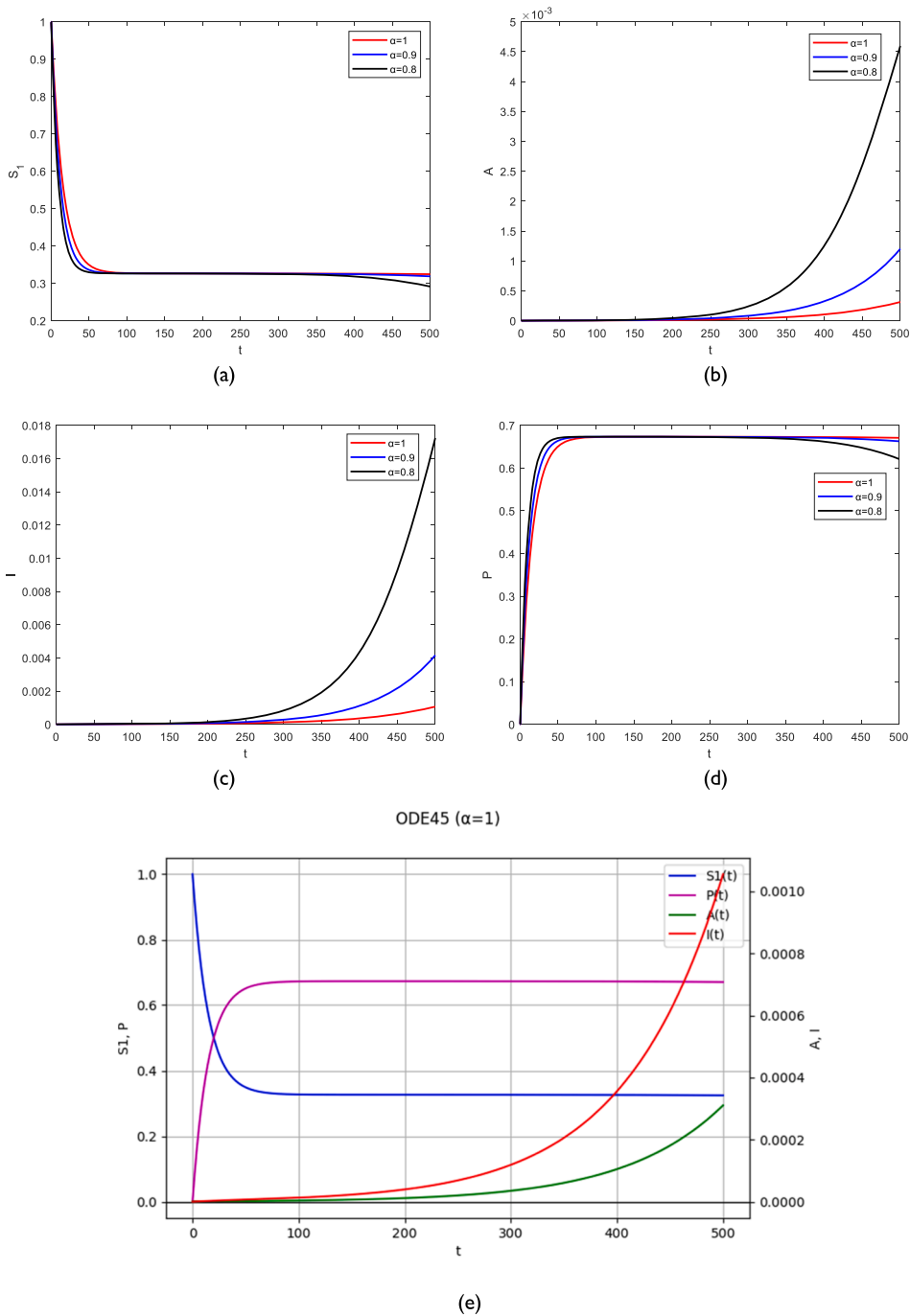


Fig. 3. Same as Fig. 2 with $\beta_2 = 0.25$, $\rho_2 = 0.55$.

those computed using MATLAB’s ODE45 for the different model categories. It is evident from these figures that the proposed method is efficient and accurate, as it perfectly agrees with the MATLAB results. Detailed numerical simulations of the model are presented in Figs. 2–4, illustrating the behavior of each compartment under these parameter variations. The figures illustrate how changes in the fractional order α , the transmission rate β , and the fraction of susceptible individuals transitioning to the protected class through treatment protocols affect the model dynamics. As shown in Fig. 2, varying the fractional order significantly influences the trajectories of the system’s compartments. For example, stabilization is achieved by decreasing the values of α , which affects the susceptible category to degenerate rapidly over time, as some control strategies are provided, ensuring that the number of the other compartments decreases similarly. Changing the values of the β and ρ , while changing the values of $\alpha = 1, 0.9, 0.8$, has a specific noticeable effect in

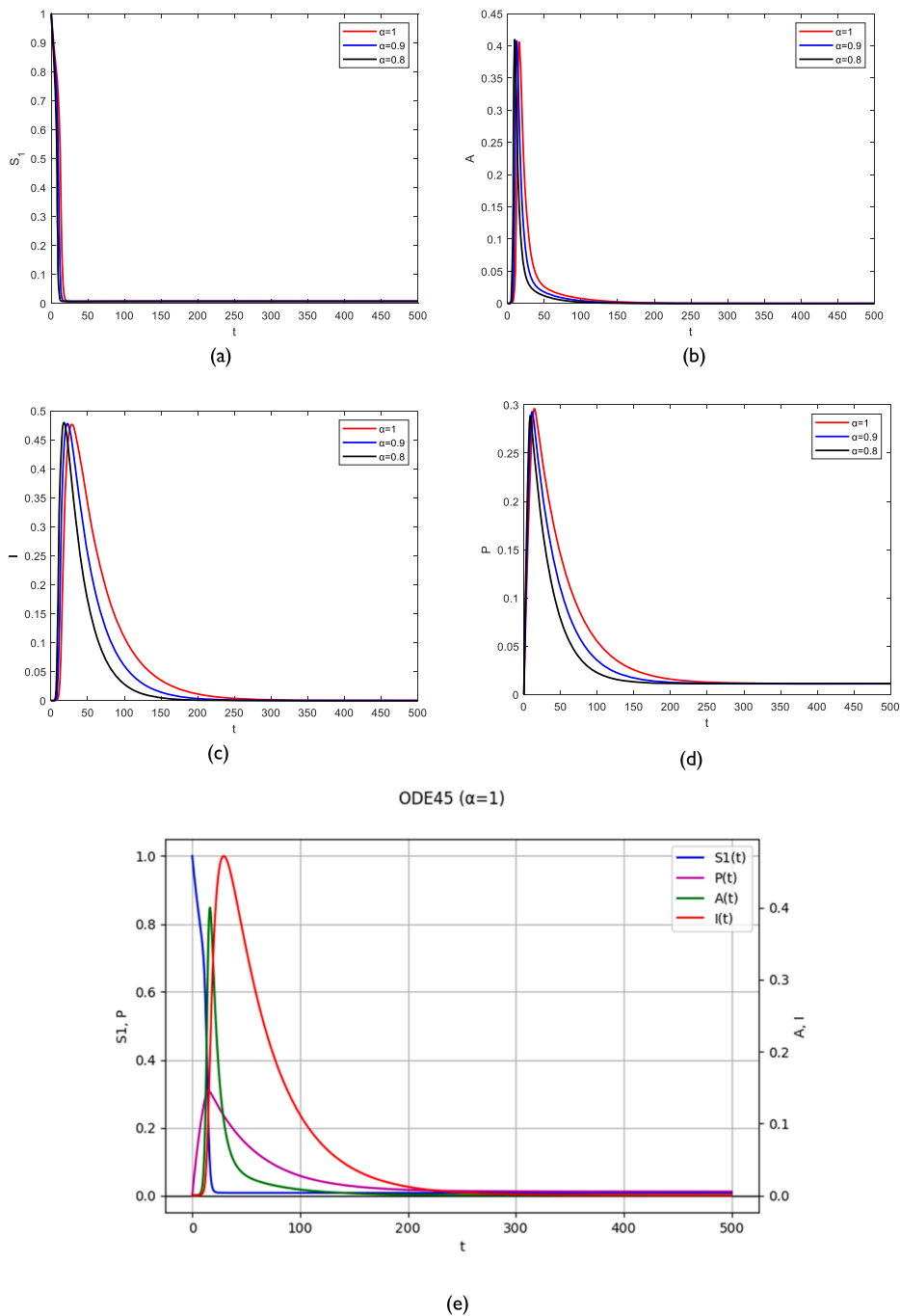


Fig. 4. Same as Fig. 2 with $\beta_3 = 1.91$, $\rho_3 = 0.4$.

Fig. 3. It can be witnessed that decreasing the transmission rates β while decreasing the value of the fractional order α affects $S(t)$ of decreased quickly, and the other compartments increased as time marched on. The asymptomatic $A(t)$ is seen to increase as more individuals re-infect, the more asymptomatic people are witnessed, and the more protected $P(t)$ are observed, even when infected, but eventually become stable. The number of infected individuals is expected to increase due to the increasing number of asymptomatic cases; thus, the silent transmission of the virus will increase the number of infected cases, which proves that the effect of the presence of the asymptomatic carrier inside the community will increase the number of infections and thus the number of protected individuals will be stable. Thus, it is crucial to emphasize the importance of controlling the number of asymptomatic carriers by implementing social distancing measures, mandating mask-wearing, and conducting continuous testing. In addition, in Fig. 4, the transmission rate β is increased while decreasing the fraction of the susceptible transferred to the protected ρ ; it is noticed that the susceptible $S(t)$ are seen

to decay faster. As for the asymptomatic $A(t)$ and protected $P(t)$, it is seen to be increasing in a short time, and this concludes that when trying to simulate system (2.1) with different values of fractional order values gives more realistic data other than when $\alpha = 1$ for the integer order, which concludes that reducing the rate of contact among individuals especially the asymptomatic will guarantee a faster decay in the infection rate and thus suppress the spread of the virus inside the community.

Real World Validation

In this subsection, we validate the results obtained from the LADM and numerical techniques by comparing them with real data from Portugal. During the early stages of 2020, specifically from March 2020, Portugal implemented its first nationwide lockdown for several facilities as a proactive measure to slow the spread of COVID-19. The number of infected (confirmed) cases per million and the number of hospitalized (Protected) cases are shown in Fig. 5. These results, reported in Fig. 5, were collected from the Our World in Data website [42]. To better capture the real data trends, we performed simulations using the LADM method over the same time interval for $0 \leq t \leq 500$. As seen in these figures, during the first lockdown period after March 2020, the number of infected and hospitalized cases began to stabilize as the government’s intervention lockdown, mask mandates, and social distancing, helped reduce the spread of the virus. According to Fig. 5, there is a clear agreement between the simulated results and the real data from Portugal. For example, Fig. 4(a) shows the number of infected cases in Portugal until July 2021. The data indicate that the number of confirmed cases initially increased, then started to decline from January 2020 until April 2020, when the first lockdown was applied, and remained lower until the end of November 2020. In Fig. 4(b), the influence of the fractional-order term is evident: varying the value of α significantly affects the stabilization of infection numbers, providing a better physical understanding of the virus’s spread dynamics. Similarly, the actual number of hospitalized/protected cases in Portugal is shown in Fig. 4(c) and compared with the simulated data in Fig. 4(d). The close fit between the two confirms that the proposed model accurately reproduces the observed trends, including the reduction in hospitalized/protected cases during the lockdown period. Overall, these results demonstrate that the proposed model aligns well with real-world data for Portugal.

Conclusion

In this study, we proposed and analyzed a fractional-order SAIP epidemic model that explicitly incorporates asymptomatic

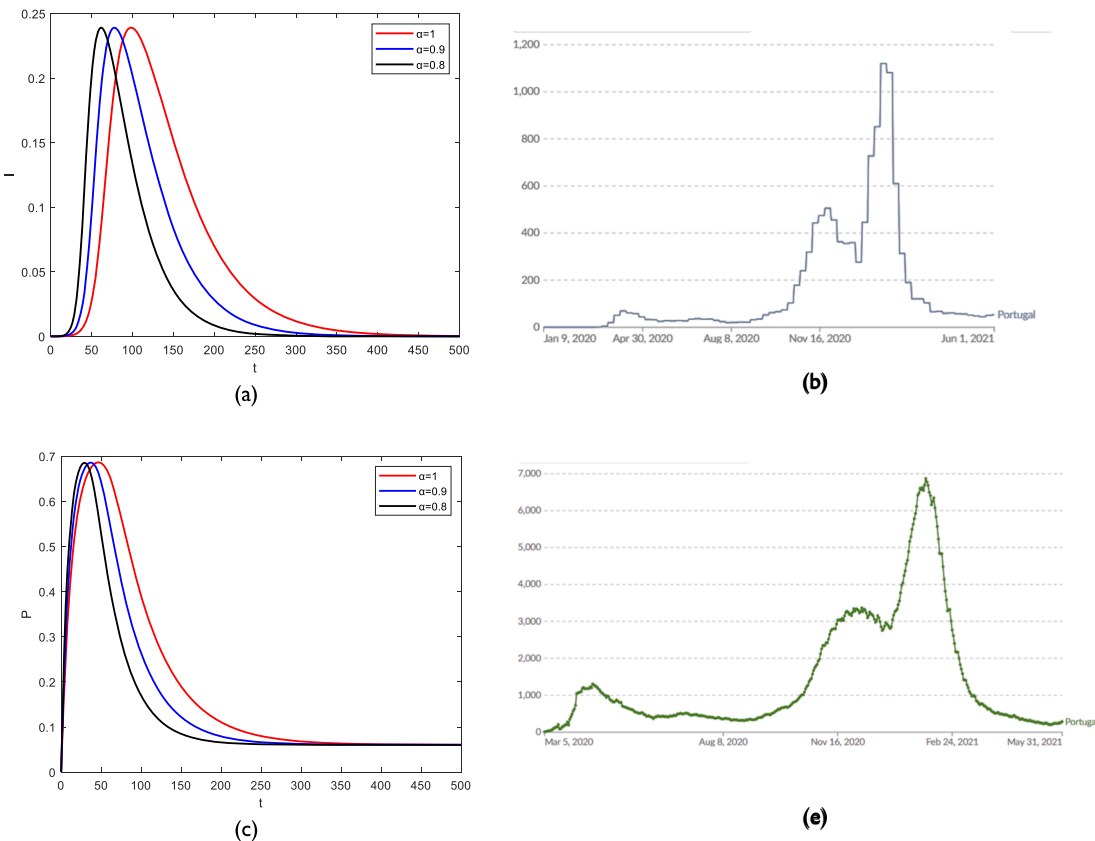


Fig. 5. (a) Number of infected cases from simulations for $\alpha = 1, 0.9, 0.8$, and (b) Number of actual confirmed cases for Portugal [42], (c) Number of protected/hospitalized cases from simulations for $\alpha = 1, 0.9, 0.8$, (d) Number of actual hospitalized cases for Portugal [42].

transmission. The model was formulated using the Caputo fractional derivative, enabling the capture of memory and hereditary effects inherent in real epidemic processes. We established key mathematical properties, proving the positivity and boundedness of solutions to ensure epidemiological validity. Moreover, we derived the basic reproduction number R_0 and conducted a rigorous analysis of the local and global stability of both the disease-free and endemic equilibria, thereby providing critical threshold conditions under which the disease either vanishes or persists. To address the complexity of the fractional system, we employed an adapted Laplace Adomian Decomposition Method (LADM) to obtain approximate analytical solutions, demonstrating its effectiveness in handling the non-local nature of fractional operators. The method's performance and convergence were illustrated through detailed graphical and tabular results, highlighting how variations in the fractional order significantly affect epidemic dynamics, including changes in peak infection sizes and outbreak duration, underscoring the crucial influence of memory effects. In addition, comparison with real-world data shows that the model provides a comprehensive and reliable simulation of confirmed and hospitalized COVID-19 cases in Portugal. For future work, we plan to extend this model by incorporating vaccination strategies, spatial structures to reflect regional heterogeneity, and stochastic effects to account for random perturbations.

Declaration of interests

The authors declare that they have no known competing financial interests or personal relationships that could have appeared to influence the work reported in this paper.

Funding

We declare that our paper is not funded.

Availability of data and materials

All data generated or analyzed during this study are included.

Acknowledgment

This study is supported via funding from Prince Sattam bin Abdulaziz University project number (PSAU/2025/R/1446). In addition, the authors would like to convey their thanks to the Editor and Reviewers for the helpful comments and suggestions that improved the work.

CRediT author statement

Hatira Günerhan: Conceptualization, Investigation, Software, Writing - original draft.
 Mohammad Sharif Ullah: Conceptualization, Methodology, Investigation, Writing - original draft.
 Kottakkaran Soopy Nisar: Formal analysis, Software, Validation, Writing - original draft, Writing - review editing.
 Waleed Adel: Investigation, Software, Validation, Writing - original draft, Writing - review editing.

References

- [1] F. Ndaïrou, I. Area, J.J. Nieto, C.J. Silva, D.F. Torres, Fractional model of COVID-19 applied to Galicia, Spain and Portugal, *Chaos, Solitons & Fractals* 144 (2021) 110652.
- [2] W.O. Kermack, A.G. McKendrick, A contribution to the mathematical theory of epidemics, *Proceedings of the royal society of london. Series A, Containing papers of mathematical and physical character* 115 (772) (1927) 700–721.
- [3] A.O. Yunus, M.O. Olayiwola, A.M. Ajileye, A Fractional Mathematical Model for Controlling and Understanding Transmission Dynamics in Computer Virus Management Systems, *Jambura Journal of Biomathematics (JJBM)* 5 (2) (2024) 116–131.
- [4] A. Zobayer, M.S. Ullah, K.M. Ariful Kabir, A cyclic behavioral modeling aspect to understand the effects of vaccination and treatment on epidemic transmission dynamics, *Scientific Reports* 13 (1) (2023) 8356.
- [5] M.S. Ullah, K.A. Kabir, Behavioral game of quarantine during the monkeypox epidemic: Analysis of deterministic and fractional order approach, *Heliyon* 10 (5) (2024) e26998.
- [6] C. Yang, J. Wang, A mathematical model for frog eye leaf spot epidemics in soybean, *Mathematical Biosciences and Engineering* 21 (1) (2023) 1144–1166.
- [7] M. Martcheva, *An introduction to mathematical epidemiology*, 61, Springer, New York, 2015, pp. 9–31.
- [8] A.O. Yunus, M.O. Olayiwola, K.A. Adedokun, J.A. Adedeji, I.A. Alaje, Mathematical analysis of fractional-order Caputo's derivative of coronavirus disease model via Laplace Adomian decomposition method, *Beni-Suef University Journal of Basic and Applied Sciences* 11 (1) (2022) 144.
- [9] J. Bai, J. Wang, Modeling long COVID dynamics: Impact of underlying health conditions, *Journal of theoretical biology* 576 (2024) 111669.
- [10] A.O. Yunus, M.O. Olayiwola, Dynamics of Ebola virus transmission with vaccination control using Caputo-Fabrizio Fractional-order derivative analysis, *Modeling Earth Systems and Environment* 11 (3) (2025) 1–18.
- [11] A.O. Yunus, M.O. Olayiwola, Epidemiological analysis of Lassa fever control using novel mathematical modeling and a dual-dosage vaccination approach, *BMC Research Notes* 18 (1) (2025) 199.
- [12] M.O. Olayiwola, A.O. Yunus, Non-integer time fractional-order mathematical model of the COVID-19 pandemic impacts on the societal and economic aspects of Nigeria, *International Journal of Applied and Computational Mathematics* 10 (2) (2024) 90.
- [13] A.O. Yunus, M.O. Olayiwola, Simulation of a novel approach in measles disease dynamics models to predict the impact of vaccinations on eradication and control, *Vacunas* 26 (2) (2025) 100385.
- [14] M.O. Olayiwola, A.O. Yunus, A. Ismaila, Alaje, J.A. Adedeji, Modeling within-host Chikungunya virus dynamics with the immune system using semi-analytical approaches, *BMC Research Notes* 18 (1) (2025) 201.

- [15] A.O. Yunus, M.O. Olayiwola, A mathematical model for assessing vaccination's efficacy as a preventative strategy against newly emerging COVID-19 variants, *Vacunat* (2025) 500392.
- [16] A.A. Elsadany, Y. Sabbar, W. Adel, A. El-Mesady, Dynamics of a novel discrete fractional model for maize streak epidemics with linear control, *International Journal of Dynamics and Control* 13 (1) (2025) 1–25.
- [17] A.O. Oladapo, A.O. Yunus, M.A. Omoloye, M.O. Olayiwola, Novel approaches to malaria control and eradication using fractional-order modeling and numerical simulations, *Next Research* 2 (2) (2025) 100205.
- [18] Michele. Caputo, Linear models of dissipation whose Q is almost frequency independent-II, *Geophysical journal international* 13 (5) (1967) 529–539.
- [19] G. Adomian, *Solving frontier problems of physics: the decomposition method* (Vol. 60), Springer Science & Business Media, 2013.
- [20] M.S. Ullah, M. Higazy, K.A. Kabir, Dynamic analysis of mean-field and fractional-order epidemic vaccination strategies by evolutionary game approach, *Chaos, Solitons & Fractals* 162 (2022) 112431.
- [21] M.O. Olayiwola, A.O. Yunus, Mathematical analysis of a within-host dengue virus dynamics model with adaptive immunity using Caputo fractional-order derivatives, *Journal of Umm Al-Qura University for Applied Sciences* 11 (2024) 104–123.
- [22] H. Günerhan, H. Dutta, M.A. Dokuyucu, W. Adel, Analysis of a fractional HIV model with Caputo and constant proportional Caputo operators, *Chaos, Solitons & Fractals* 139 (2020) 110053.
- [23] M.S. Ullah, M. Higazy, K.A. Kabir, Modeling the epidemic control measures in overcoming COVID-19 outbreaks: A fractional-order derivative approach, *Chaos, Solitons & Fractals* 155 (2022) 111636.
- [24] M.O. Olayiwola, A.I. Alaje, A.O. Yunus, A Caputo fractional order financial mathematical model analyzing the impact of an adaptive minimum interest rate and maximum investment demand, *Results in Control and Optimization* 14 (2024) 100349.
- [25] A.O. Yunus, M.O. Olayiwola, Mathematical modeling of malaria epidemic dynamics with enlightenment and therapy intervention using the Laplace-Adomian decomposition method and Caputo fractional order, *Franklin Open* (2024) 100147.
- [26] M.Y. Ongun, The Laplace Adomian decomposition method for solving a model for HIV infection of CD4+ T cells, *Mathematical and Computer Modelling* 53 (5-6) (2011) 597–603.
- [27] A.O. Yunus, M.O. Olayiwola, The analysis of a co-dynamic ebola and malaria transmission model using the laplace adomian decomposition method with caputo fractional-order, *Tanzania Journal of Science* 50 (2) (2024) 224–243.
- [28] F. Haq, K. Shah, G. ur Rahman, M. Shahzad, Numerical solution of fractional order smoking model via Laplace Adomian decomposition method, *Alexandria Engineering Journal* 57 (2) (2018) 1061–1069.
- [29] A.O. Yunus, M.O. Olayiwola, M.A. Omoloye, A.O. Oladapo, A fractional order model of lassa disease using the Laplace-adomian decomposition method, *Healthcare Analytics* 3 (2023) 100167.
- [30] D. Baleanu, S.M. Atyad, H. Mohammadi, S. Rezapour, On modelling of epidemic childhood diseases with the Caputo-Fabrizio derivative by using the Laplace Adomian decomposition method, *Alexandria Engineering Journal* 59 (5) (2020) 3029–3039.
- [31] O. González-Gaxiola, A. Biswas, Optical solitons with Radhakrishnan–Kundu–Lakshmanan equation by Laplace–Adomian decomposition method, *Optik* 179 (2019) 434–442.
- [32] A.O. Yunus, M.O. Olayiwola, The analysis of a novel COVID-19 models with the fractional-order incorporating the impact of the vaccination campaign in Nigeria via the Laplace-Adomian Decomposition Method, *Journal of the Nigerian Society of Physical Sciences* (2024) 1830.
- [33] H. Günerhan, M. Kaabar, E. Celik, Novel analytical and approximate-analytical methods for solving the nonlinear fractional smoking mathematical model, *Sigma Journal of Engineering and Natural Sciences* 41 (2) (2023) 331–343.
- [34] M.O. Olayiwola, A.I. Alaje, A.O. Yunus, K.A. Adedokun, K.A. Bashiru, A mathematical modeling of COVID-19 treatment strategies utilizing the Laplace Adomian decomposition method, *Results in Control and Optimization* 14 (2024) 100384.
- [35] A. Abdullahi, Modelling of transmission and control of Lassa fever via Caputo fractional-order derivative, *Chaos, Solitons & Fractals* 151 (2021) 111271.
- [36] Y. Zhang, X. Yu, H. Sun, G.R. Tick, W. Wei, B. Jin, Applicability of time fractional derivative models for simulating the dynamics and mitigation scenarios of COVID-19, *Chaos, Solitons & Fractals* 138 (2020) 109959.
- [37] Herrmann, R. (2011). *Fractional calculus: an introduction for physicists*.
- [38] C.J. Silva, C. Cruz, D.F. Torres, A.P. Munuzuri, A. Carballosa, I. Area, J. Mira, Optimal control of the COVID-19 pandemic: controlled sanitary deconfinement in Portugal, *Scientific reports* 11 (1) (2021) 3451.
- [39] A. Atangana, S. İğret Araz, Modeling and forecasting the spread of COVID-19 with stochastic and deterministic approaches: Africa and Europe, *Advances in Difference Equations* 2021 (2021) 1–107.
- [40] F. Brauer, C. Castillo-Chavez, C. Castillo-Chavez, *Mathematical models in population biology and epidemiology* (Vol. 2, No. 40), Springer, New York, 2012.
- [41] S.O. Edeki, T. Motsepa, C.M. Khalique, G.O. Akinlabi, The Greek parameters of a continuous arithmetic Asian option pricing model via Laplace Adomian decomposition method, *Open Physics* 16 (1) (2018) 780–785.
- [42] <https://ourworldindata.org/explorers/covid>.